Nuclear Engineering and Technology xxx (xxxx) xxx

Contents lists available at ScienceDirect

Nuclear Engineering and Technology

journal homepage: www.elsevier.com/locate/net

A spent nuclear fuel source term calculation code BESNA with a new modified predictor-corrector scheme

Duy Long Ta [a], Ser Gi Hong [a, *], Dae Sik Yook [b]

[a] Department of Nuclear Engineering, Hanyang University, 222 Wangsimni-ro, Seongdong-gu, Seoul, 04763, South Korea
[b] Korea Institute of Nuclear Safety (KINS), 62 Gwahak-ro, Yuseong-gu, Daejon, South Korea

ARTICLE INFO

Article history:
Received 12 April 2022
Received in revised form
15 June 2022
Accepted 18 July 2022
Available online xxx

Keywords:
Depletion calculation
Source term
CRAM
Matrix exponential
BESNA

ABSTRACT

This paper introduces a new point depletion-based source term calculation code named BESNA (Bateman Equation Solver for Nuclear Applications), which is aimed to estimate nuclide inventories and source terms from spent nuclear fuels. The BESNA code employs a new modified CE/CM (Constant Extrapolation – Constant Midpoint) predictor-corrector scheme in depletion calculations for improving computational efficiency. In this modified CE/CM scheme, the decay components leading to the large norm of the depletion matrix are excluded in the corrector, and hence the corrector calculation involves only the reaction components, which can be efficiently solved with the Talyor Expansion Method (TEM). The numerical test shows that the new scheme substantially reduces computing time without loss of accuracy in comparison with the conventional scheme using CRAM (Chebyshev Rational Approximation Method), especially when the substep calculations are applied. The depletion calculation and source term estimation capability of BESNA are verified and validated through several problems, where results from BESNA are compared with those calculated by other codes as well as measured data. The analysis results show the computational efficiency of the new modified scheme and the reliability of BESNA in both isotopic predictions and source term estimations.

1. Introduction

The accurate prediction of the nuclide compositions during burn-up or irradiation is essential in many nuclear engineering problems, such as the source term estimation for criticality and shielding calculations, radioactivity, and heat generation. So far, various numerical methods have been proposed for depletion and decay calculations, which can be categorized into three main types: The numerical approaches for the system of differential equations, such as the Runge-Kutta method and the Gear's method [1,2], the Transmutation Trajectory Analysis (TTA) method [3,4], and the matrix exponential methods [5–11]. Among them, the TTA and the matrix exponential methods are more prevalent in complex depletion problems, while the first approach is generally not suitable due to the stiffness of the equations. In depletion calculation with the TTA method, the depletion system is decomposed into a set of linear reaction chains where the concentration for each nuclide in a linear reaction chain can be obtained by an analytical solution. On the other hand, the system of differential depletion equations is represented in the matrix-vector form in the matrix exponential methods. The matrix exponential methods use numerous approaches [5] to approximate the matrix exponential but only a few of them can be applied in depletion calculation due to the characteristic of the depletion matrix. Among these approaches, the Taylor Expansion Method (TEM) used in ORIGEN2 and SCALE/ORIGEN has very good computational speed, but it requires the norm of the depletion matrix to be sufficiently small. Because of this limitation, the short-lived nuclides which contribute to a large norm of the depletion matrix should be removed from the depletion matrix and calculated with an alternative method. Recently, CRAM has been introduced in depletion calculations [12,13] with both good computational accuracy and efficiency. Compared to the TEM method, CRAM calculation takes a longer computing time, but it can provide more reliable results with the capability to directly treat the short-lived nuclides without removing them from the depletion matrix.

In practical problems with nuclear fuel, the system power is generally assumed to be constant during a given time step rather

* Corresponding author., Department of Nuclear Engineering, Hanyang University, 222 Wangsimni-ro, Seongdong-gu, Seoul, 04763, South Korea.
E-mail address: hongsergi@hanyang.ac.kr (S.G. Hong).

https://doi.org/10.1016/j.net.2022.07.013

than the neutron flux. Since the numerical methods in depletion calculations require a constant neutron flux used in each step, the predictor-corrector schemes [12–14] have been typically used to calculate the step-average flux representing the step-average power. Conventionally, the calculations in predictor and corrector use the same form of depletion equation where the corrector uses the step-average flux calculated from the predictor. Thus, the same numerical method is used in both predictor and corrector calculations. In this paper, the authors suggest a new modified form of the CE/CM predictor-corrector scheme where the corrector calculation can be performed without the decay components. By using this scheme, the norm of the calculation matrix in the corrector becomes sufficiently small, so the TEM method can be used with very good computational efficiency. This new method was implemented in the stand-alone point depletion-based source term code BESNA.

The stand-alone point depletion code BESNA has been developed recently by the authors for various purposes, including the estimation of nuclide inventories and source terms such as decay heat, radioactivities, and radiation emission spectra from spent nuclear fuels and irradiated structural materials. The BESNA code is developed as a new depletion and activation calculation module with high computational efficiency which will be used as the main solver in our in-house automatic source term generation system for huge number of spent fuel assemblies and in our in-house activation analysis system coupled with multi-group transport calculations. In BESNA, the substep calculations are also employed with the flux renormalization method [15] implemented in SCALE/ORIGEN. The changes of cross sections during burnup, which are typically treated in coupled depletion codes [12–14,16–20], are also considered in BESNA by using the self-adaptive burnup-dependent effective one-group cross sections generated by MCNP6 based on ENDF/B-VII.1 cross section data. This paper summarizes our work on development as well as verification and validation of the BESNA code. Section 2 describes the calculation algorithm, including the description of methods and the data libraries used in BESNA. Section 3 provides the verification and validation of the BESNA code for the isotopic predictions and source term estimations. Finally, the conclusions are presented in Section 4.

2. Theory and methods

2.1. Review of the numerical methods used in BESNA

In this subsection, the numerical methods employed in BESNA depletion calculations are reviewed. The change rate of atomic density for a nuclide i in a mixture can be calculated by solving the following Bateman equation:

$$\frac{dn_i}{dt} = (-\lambda_i - \sigma_i\phi)n_i + \sum_{j=1, j\neq i}^{N} (\lambda_j b_{j,i} + \sigma_{j,i}\phi)n_j + \sum_{k=1}^{L} \sigma_{f,k}\gamma_{k,i}\phi n_k \quad (1)$$

where n_i is the concentration of nuclide i, λ_i is the decay constant of nuclide i, $b_{j,i}$ is the decay branching of nuclide j which results nuclide i, ϕ is the one-group total neutron flux, σ_i is the total microscopic effective one-group removal cross section of nuclide i, $\sigma_{j,i}$ is the microscopic effective one-group cross section of the reactions of nuclide j which results nuclide i. In Eq. (1), $\sigma_{f,k}$ and $\gamma_{k,i}$ are the effective one-group fission cross section of nuclide k and its fission yield which results nuclide i, respectively, while N and L are the numbers of nuclides and fission source nuclides in the mixture, respectively.

Actually, Eq. (1) represents a system of the first-order differential equations, which can be written in the following matrix-vector form:

$$\frac{d\vec{N}(t)}{dt} = A\vec{N}(t) \quad (2)$$

where $\vec{N}(t)$ is the vector of nuclide concentrations and A is the depletion matrix. The formal solution of Eq. (2) can be expressed as the following matrix exponential form:

$$\vec{N}_t = e^{tA}\vec{N}_0 \quad (3)$$

where $\vec{N}_0$ represents the vector of initial nuclide concentrations. The CRAM method uses the rational approximation of the matrix exponential, especially near the negative real axis [5]. The solution of Eq. (3) can be expressed using CRAM in partial fraction decomposition form as

$$\vec{N}_t = \alpha_0\vec{N}_0 + 2Re\sum_{i=1}^{k/2}(tA - \theta_i I)^{-1}\alpha_i\vec{N}_0 \quad (4)$$

where k is the order of the approximation, α_0 is the limit of the rational function at infinity and α_i is the residues at the poles θ_i of the rational function.

The second term in the right hand side of Eq. (4) can be separated into $k/2$ independent terms, where the calculation of $(tA - \theta_i I)^{-1}\vec{N}_0$ is required. Each vector $(tA - \theta_i I)^{-1}\vec{N}_0$ in Eq. (4) can be calculated by solving the following system of equations:

$$(tA - \theta_i I)\vec{x}_i = \vec{N}_0 \quad (5)$$

In BESNA, Eq. (5) is separately set up for each group of nuclides: activations, actinides, and fission products. The system of equations for each group is solved in BESNA using the Gauss-Seidel method. The systems of equations for activation and actinide nuclides are solved independently, and then the system of equations for fission products is solved using the concentration of actinide nuclides. In our depletion code BESNA, the CRAM method with orders of 14 and 16 was implemented [21]. Nowadays, CRAM is considered the best numerical method in depletion calculations for nuclear fuel, with the ability to give an accurate solution to the burnup equations with a short computing time. However, the computational speed of CRAM is a deficiency in comparison with TEM method in SCALE/ORIGEN. The TEM method represents Eq. (3) with the Taylor expansion of the matrix exponential as follows:

$$\vec{N}_t = \left[I + tA + \frac{(tA)^2}{2} + \ldots\right]\vec{N}_0 \quad (6)$$

In the TEM method, only a finite number of terms (i.e., L) in Eq. (6) is considered and the right hand side of Eq. (6) with only L terms is calculated using a recursion relation [13]:

$$\vec{N}_t = \sum_{n=0}^{L}\vec{C}_n \quad (7)$$

where $\vec{C}_0 = \vec{N}_0$, $\vec{C}_{n+1} = \frac{t}{n+1}A\vec{C}_n$. The use of the TEM method with this recursion relation requires storage of only two vectors $\vec{C}_n$ and $\vec{C}_{n+1}$. To compute the matrix exponential by the Taylor expansion with double-precision arithmetic with the TEM method, the following constraint on the matrix norm has been chosen in depletion codes:

$$[A]t \leq -2\ln(0.001) = 13.8155 \tag{8}$$

The matrix norm in Eq. (8) is defined as the smallest one of themaximum-row absolute sums and the maximum-column absolute sums [13]:

$$[A] = min\left\{\max_j \sum_i |a_{ij}|, \max_i \sum_j |a_{ij}|\right\} \tag{9}$$

The matrix norm may exceed this value in practical problems due to the short-lived nuclides having large decay constants. Therefore, the depletion calculations using the TEM method may require a much shorter time step than those using CRAM and removals of the short-lived nuclides from the depletion matrix.

2.2. Numerical approaches in depletion calculation with BESNA

The depletion module in BESNA provides two calculation modes: 1) Irradiation calculation with the constant flux given in each step and 2) Burnup calculation with the fixed power given in each step. In BESNA, the effective one-group cross sections used in each desired burnup are generated by linear interpolation from the prepared cross sections at two nearest neighboring burnups available in the library, which is described in subsection 2.4.

In depletion calculations, the BESNA code uses the CE/CM predictor-corrector scheme to estimate step-average flux with given power by using two approaches, which are named as the conventional approach and the modified one suggested in this work. The predictor calculation in both of these approaches is performed by solving the depletion equation with the beginning of step (BOS) cross sections and flux as follows:

$$\overrightarrow{N}_t^{pred} = e^{t\left(A^d + A^r_{BOS}\phi_{BOS}\right)}\overrightarrow{N}_0 \tag{10}$$

where $\overrightarrow{N}_t^{pred}$ is the predicted nuclide concentration vector at the end of step (EOS), and the superscripts d and r are used to represent the decay and reaction matrices, respectively.

In BESNA, the predictor calculation is performed by CRAM. After performing the predictor calculation, the predicted EOS flux (ϕ_{EOS}^{pred}) can be calculated by using the cross sections corresponding to the EOS burnup. Then the flux at the middle of step (MOS), which represents the step-average flux in the CE/CM scheme, is estimated as the average of the BOS and predicted EOS fluxes as follows:

$$\phi_{MOS} = \frac{1}{2}\left[\phi_{BOS} + \phi_{EOS}^{pred}\right] \tag{11}$$

In the conventional approach, the corrector calculation is performed using CRAM by solving Eq. (10) with the MOS cross sections and flux:

$$\overrightarrow{N}_t = e^{t\left(A^d + A^r_{MOS}\phi_{MOS}\right)}\overrightarrow{N}_0 \tag{12}$$

On the other hand, for the corrector calculation with the modified approach, we rewrite Eq. (12) using the reaction matrix term at BOS as follows:

$$\overrightarrow{N}_t = e^{t\left(A^r_{MOS}\phi_{MOS} - A^r_{BOS}\phi_{BOS}\right)} e^{t\left(A^d + A^r_{BOS}\phi_{BOS}\right)}\overrightarrow{N}_0 \tag{13}$$

It can be seen that the last exponential term on the right-hand side of Eq. (13) are the same as the right-hand side of Eq. (10), which results in the predicted nuclide concentration vector at the EOS. For that reason, the corrector calculation can be performed by solving:

$$\overrightarrow{N}_t = e^{t\left(A^r_{MOS}\phi_{MOS} - A^r_{BOS}\phi_{BOS}\right)}\overrightarrow{N}_t^{pred} \tag{14}$$

At this stage, the decay matrix A^d is excluded from the corrector calculation. By removing the decay matrix from the calculation, the norm of the matrix becomes smaller because the large norm of the depletion matrix is contributed by the short-lived nuclides which have very large decay constants [13]. So that, the corrector calculation in the modified approach can be efficiently performed by the TEM method rather than CRAM method.

Additionally, the renormalization methods can be applied in corrector calculation to consider the flux change due to the change of nuclide concentrations during each step. The renormalization process is usually performed by dividing a time step into several substeps, and the flux used in each substep then be recalculated. Several renormalization methods can be used in substep calculations, such as beginning-of-substep renormalization (BOSS), middle-of-substep renormalization (MOSS), or the approach used in ORIGEN for substep calculation [20]. The substep calculation with flux renormalization is also implemented in BESNA using approach used in ORIGEN [20,22], where the flux in each substep is obtained by multiplying step-average flux with a renormalization factor given by the following equation:

$$\Phi_s = \frac{P}{\sum_i \left(\kappa_{f,i}\sigma_{f,i} + \kappa_{c,i}\sigma_{c,i}\right)\overline{\phi} V n_{s,i}} \tag{15}$$

where

P is the given system power.

i is the nuclide index.

$\kappa_{f,i}$ and $\kappa_{c,i}$ are the recoverable energies per fission and capture of nuclide i, respectively,

$\sigma_{f,i}$ and $\sigma_{c,i}$ are the one group fission and capture cross sections of nuclide i, respectively,

$\overline{\phi}$ is the step-average flux,

V is the volume of mixture,

$n_{s,i}$ is the number density of nuclide i at the beginning of substep s.

When the substep calculations are applied in the corrector, Eq. (14) is rewritten as follows:

$$N_t = \prod_{s=1}^{N_s} e^{\frac{t}{N_S}\left(A^r_{MOS}\phi_{MOS}\Phi_s - A^r_{BOS}\phi_{BOS}\right)} N_t^{pred} \tag{16}$$

where N_s is the number of substeps. In this case, the evaluations for the N_s matrix exponentials in Eq. (16) are performed using the TEM method. On the other hand, in the conventional scheme, the corrector calculation with substep is performed by solving the following equation:

$$N_t = \prod_{s=1}^{N_s} e^{\frac{t}{N_S}\left(A^d + A^r_{MOS}\phi_{MOS}\Phi_s\right)} N_0 \tag{17}$$

2.3. Source terms calculation in BESNA

Besides the depletion calculation module, BESNA includes other modules where the nuclide concentrations calculated by the depletion module are incorporated with the nuclear decay data to generate the source terms. The source terms calculated in BESNA include the decay heat, photon and neutron emission intensities as well as spectra with a user-defined energy group structure [13,23,24]. The decay heat from each nuclide is calculated by

multiplying the decay heat recoverable (Q_i) per decay by the nuclide number density (N_i) and the decay constant (λ_i) as shown in the following equation:

$$H = \sum_i N_i \lambda_i Q_i \tag{18}$$

where subscript i represents each unstable nuclide in the mixture.

Additionally, the contribution from spontaneous fission which was not included in the decay heat recoverable per decay (Q_i) is calculated using a value of 200 MeV per fission [13].

The photon data includes the line-energy and intensity data for the X-rays, gamma from decay, spontaneous fission gamma, (α, n) reaction gamma, and bremsstrahlung from negatron and positrons slowing down in the UO_2 mixture. The photon spectra calculation module in BESNA adjusts the data provided in the library into the user-defined energy grid to calculate the photon emission spectra using interpolation schemes.

The neutron emission source considers the contributions from (α, n) reaction and spontaneous fission. The alpha particles emitted by the decay of actinides slow down and interact with light nuclides in the medium, leading to neutrons emission. The probability of producing a neutron by a target nuclide i with atom density N_i from an alpha particle of energy E_α in a homogeneous mixture can be determined by [23,24].

$$P_i(E_\alpha) = \frac{N_i}{N} \int_0^{E_\alpha} \frac{\sigma_i(E)}{\varepsilon(E)} dE \tag{19}$$

where $\varepsilon(E)$ is the total stopping power of the mixture, $\sigma_i(E)$ is the (α, n) reaction cross section of target nuclide, and N is the total atom number density of the mixture.

Eq. (19) is numerically solved for each energy alpha particle produced from decay of actinide nuclides, and the neutron intensity from a nuclide i in a mixture via (α, n) reactions is calculated by multiplying $P_i(E_\alpha)$ with the alpha source strength as follows:

$$S^i_{\alpha,n} = N_i \lambda_i^\alpha P_i(E_\alpha) \tag{20}$$

where λ_i^α is the α decay constant of nuclide i.

The neutron spectra from (α, n) reactions are calculated by nuclear reaction kinematics with an assumption that neutrons are isotropically emitted in the center-of-mass system of α particle and target nuclide. With that assumption, the mass, momentum, and energy conservations are applied to obtain the minimum and maximum permissible energies of the emitted neutron for each product nuclide energy level [23,24]. The Q-value for each reaction, the excitation energy of the product nuclide level, and the product nuclide level branching fraction used for calculating neutron spectra from (α, n) reactions are given in the library. The neutron spectra resulting from the spontaneous fission of actinides are calculated using the Watt fission spectrum as follows:

$$N(E) = Ce^{-E/a} sinh\sqrt{bE} \tag{21}$$

where a and b are the Watt spectrum parameters, C is the normalization constant and E is the neutron energy.

2.4. Data library used in depletion calculation with BESNA

In this subsection, the data libraries used in our depletion calculations, which include the decay data, one-group cross sections, and fission yield library are described. The decay data consists of general information such as nuclide type (activation, actinide, and fission product group of nuclides), decay constant, decay heat recoverable energy, and decay branching ratios. Eleven decay types are currently considered in BESNA as follows: β^- or β^+ (or electron capture) decay resulting production nuclide in the ground or isomer state, double β^- decay, β^- decay with the emission of an α particle, α decay, isomeric transition, spontaneous fission, neutron decay, and delayed neutron decay (neutron plus β^-). These data are provided for 2237 nuclides, which are from SCALE/ORIGEN library or ENDF/B data, where several isotopes can exist in several groups for the independence of each group of nuclides.

The effective one-group cross section library used in BESNA is generated by MCNP6 [14] depletion calculations with the reaction rate and flux tallies for pin-cell and fuel assembly (FA) models. The one-group cross sections are calculated for all the nuclides having the ENDF-B/VII.1 cross section data available in MCNP6. At present, the following reactions: (n, γ), $(n, 2n)$ to ground or isomer state, (n, α), (n, p), (n, d), (n, t), $(n, 3n)$ and *(n, fission)* are considered in the BESNA cross section library. In our library, the cross sections for the reactions producing the products at the isomer state are calculated by combining the 63-group fluxes from MCNP6 at various burnups with the branching ratios calculated from the CINDER library [25], where the 63-group cross sections are provided for those reactions. The BESNA library stores the effective one-group cross section for these reactions at the different burnups, and those at a desired burnup can be calculated by using linear interpolation between the two nearest neighboring burnups in the library.

The fission yield library used in BESNA is prepared from the fission yield data given in SCALE, which are based on ENDF/B-VII.1, or can be directly from ENDF/B data. The fission yield data include fission yields of 1151 fission products for 30 fissionable actinide nuclides at energies of 0.0253 eV, 2 MeV, and 14 MeV. The fission yield data used in BESNA is calculated by weighting the fission yield data from SCALE with 63-group neutron fluxes from MCNP6 for each fissionable actinide nuclide given in Table 1.

3. Verification and validation results

3.1. CRAM solver verification with comparison to ORIGEN2

First, the CRAM solver used in the BESNA code is verified by comparing with the results calculated by ORIGEN2 for a simple homogeneous test problem. The predictor-corrector scheme in BESNA was not used in this verification of the CRAM solver through comparison with ORIGEN2, because ORIGEN2 did not implement any predictor-corrector scheme. The predictor-corrector scheme in BESNA will be used from the second problem, where the BESNA results are compared with the results from the other codes and experimental measured data. In this problem, we consider a homogeneous mixture of UO_2 with a volume of 0.536 cm^3. The atomic number densities of nuclides in the mixture are given in Table 2. The calculations with ORIGEN2 and BESNA are performed with the constant power of 1.77×10^{-4} MW up to 500 days, corresponding to the burnup of 17.1 GWd/tHM. In order to verify the CRAM solver used in the BESNA code, the same effective one-group cross section library was used both in BESNA and ORIGEN2 calculations to avoid the errors which can be occurred by differences in the cross section

Table 1
List of fission source nuclides using in BESNA.

^{227}Th	^{229}Th	^{232}Th	^{231}Pa	^{232}U	^{233}U
^{234}U	^{235}U	^{236}U	^{237}U	^{238}U	^{237}Np
^{238}Np	^{238}Pu	^{239}Pu	^{240}Pu	^{241}Pu	^{242}Pu
^{241}Am	^{242m}Am	^{243}Am	^{242}Cm	^{243}Cm	^{244}Cm
^{245}Cm	^{246}Cm	^{248}Cm	^{249}Cf	^{251}Cf	^{254}Es

Table 2
Material compositions for the homogeneous test problem 1.

Nuclide	Atomic density (atom/barn.cm)
^{235}U	1.05056E-03
^{238}U	2.33403E-02
^{16}O	4.89084E-02

library. The calculations in this problem are performed with 140 time steps where one day is used as a time step size in the first 50 steps, and step size of five days is applied for the remaining steps. Figs. 1 and 2 show the relative discrepancies in the atomic number densities estimated by BESNA in comparison with ORIGEN2 for several actinides and fission products, respectively. These figures show the atomic number densities calculated by BESNA have very good agreements compared to those by ORIGEN2, where the relative discrepancies at 100 days are less than 0.4% for all the considered nuclides and those at the final step are less than 0.1%, which means that CRAM is successfully implemented in BESNA.

3.2. Validation with the measured samples from Takahama-3 reactor

To validate the nuclide concentrations calculated with BESNA, we considered ten measured samples from the fuel assemblies (FAs) with IDs NT3G23 and NT3G24 in the Takahama-3 reactor [26]. The radial configuration of these FAs and the locations of the measured fuel rods are given in Fig. 3, where five samples are taken from fuel rod SF95 of the NT3G23 FA and the remaining ones are from the fuel rod SF97 in NT3G24 FA. These FAs have the same configuration where the UO_2 fuel rods have the initial enrichment of 4.11 wt% ^{235}U and the fuel density of 10.412 g/cm^3. Five samples from the SF95 fuel rod are measured at the shutdown time after two cycles (Cycle 5 and 6) with the burnups ranging from 14.3 GWd/tHM to 36.69 GWd/tHM. On the other hand, for the samples from the SF97 fuel rod, samarium isotopes are measured at a cooling time of 3.96 years after shutdown while other isotopes are measured at the shutdown time after three cycles (Cycles 5-7). For the SF97 fuel rod, we considered five samples (samples 2-6) with similar axial levels compared to the samples from the SF95 fuel rod.

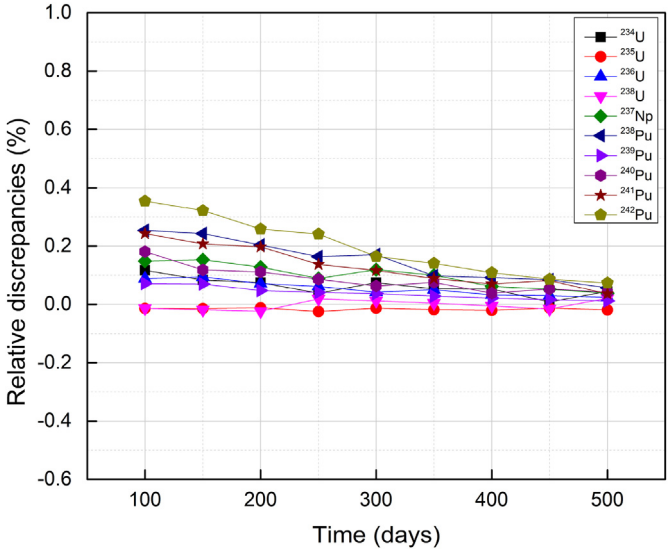

Fig. 1. Relative discrepancies (%) of BESNA to ORIGEN2 for major actinide nuclides in the homogeneous test problem.

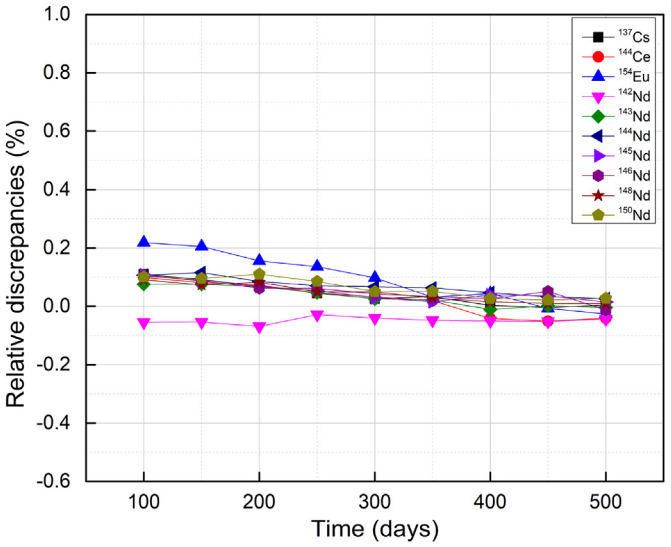

Fig. 2. Relative discrepancies (%) of BESNA to ORIGEN2 for some fission products nuclides in the homogeneous test problem.

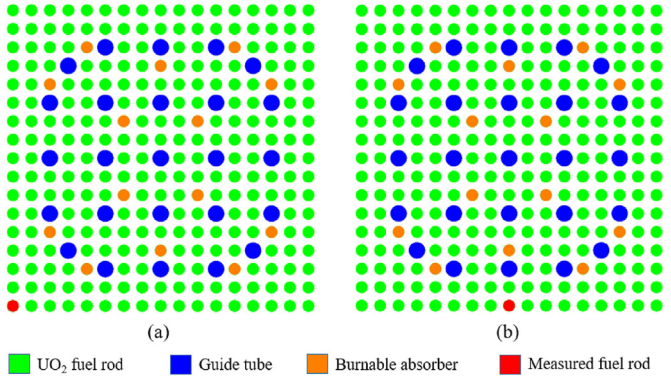

Fig. 3. Radial layout of NT3G23 (a) and NT3G24 (b) FAs of Takahama-3 reactor.

The detailed discharged burnups of the samples from these fuel rods are given in Table 3. In this test problem, the fuel pin model with reflective boundary conditions was used with consideration of the detailed specific power and boron concentration at each burnup step taken from [26]. The effective one-group cross sections for BESNA were calculated with MCNP6 for this fuel pin cell model. The calculation results from BESNA, SCALE/TRITON, and MCNP6 are inter-compared with the measurement data and the results are presented using the calculation-to-experiment ratio (C/E). Fig. 4 compares the C/E ratios calculated by MCNP6, TRITON, and

Table 3
Burnup data of fuel samples from Takahama-3 reactor.

Fuel rod	Sample	Estimated burnup (GWd/tHM)
SF95	1	14.30
	2	24.35
	3	35.42
	4	36.69
	5	30.40
SF97	2	30.73
	3	42.16
	4	47.03
	5	47.25
	6	40.79

BESNA for two representative samples of SF95 fuel rod, while the mean C/E ratios for five SF95 fuel rod samples are shown in Fig. 5.

As can be seen from these figures, the C/E ratios for nuclides in the fuel rod SF95 samples are mostly within the ±20% error boundary and the discrepancies between the different codes are within 7% for the major actinides and fission products. The C/E ratios for BESNA results also showed similar trends and similar levels with those by SCALE/TRITON and MCNP6. In particular, the large discrepancies of BESNA compared to MCNP6 and SCALE/TRITON were found for ^{245}Cm, which are 5.7% and 17.2%, respectively. The large relative discrepancies of ^{245}Cm concentration compared to TRITON may come from the differences in the effective one-group cross sections. In Fig. 6, the C/E ratios for two representative samples (samples 3 and 4) which have similar axial levels to the representative cases of SF95 are presented. The mean C/E ratios over five SF97 fuel rod samples are given in Fig. 7.

Similar to the SF95 fuel rod samples, the C/E ratios for the SF97 fuel samples are mostly within the ±20% error boundary with similar trends and similar levels from BESNA compared to the reference depletion codes. For the actinide nuclides, the largest error occurs for ^{245}Cm, where the relative discrepancies compared to MCNP6 and TRITON are 5.6% and 15.2%, respectively. The results for fission products also showed good agreements between BESNA and the references codes except for ^{148}Sm. For this nuclide, it is noted that BESNA and MCNP6 give the similar level of discrepancies from the measurements while BESNA overestimates but MCNP6 underestimates it. The relatively large discrepancy of BESNA compared to TRITON for ^{148}Sm may be contributed by the use of burnup-independent fission yield in the BESNA code. The results in this validation problem leads to the conclusion that BESNA gives good agreements with the reference codes (MCNP6 and TRITON) which use the coupling of transport and depletion calculations and the discrepancies from measurements are also similar to the reference codes except for few nuclides.

For this problem, the computational efficiency of the new modified predictor-corrector scheme in BESNA where CRAM and TEM are used in the predictor and corrector, respectively, was also tested by comparing the computing times and relative discrepancies in nuclide concentrations with the traditional CE/CM method using CRAM. The maximum relative discrepancy of the atomic number densities estimated with the new modified

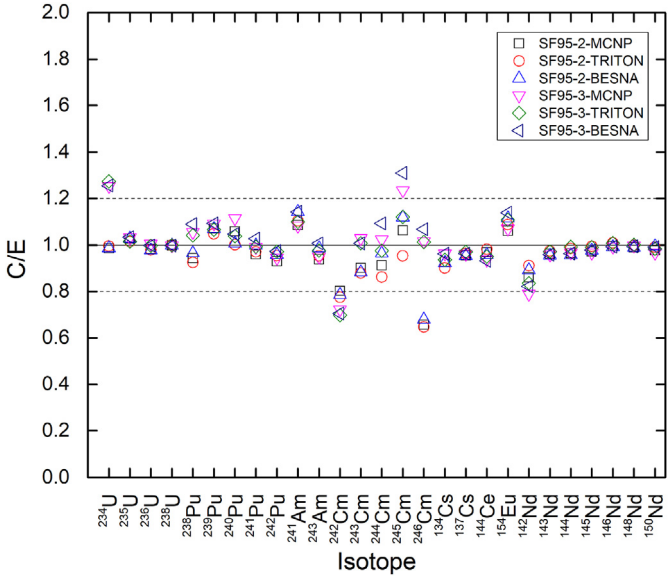

Fig. 4. Comparison of C/E ratios for samples 2 and 3 of fuel rod SF95.

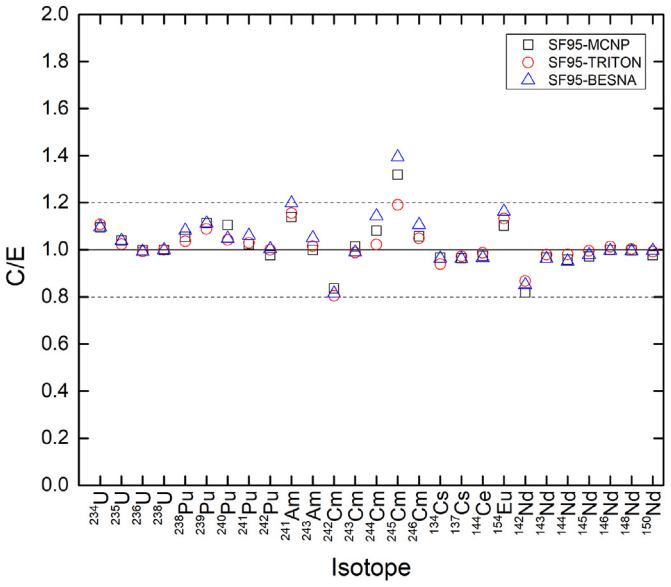

Fig. 5. Comparison of the mean C/E ratio for SF95 samples.

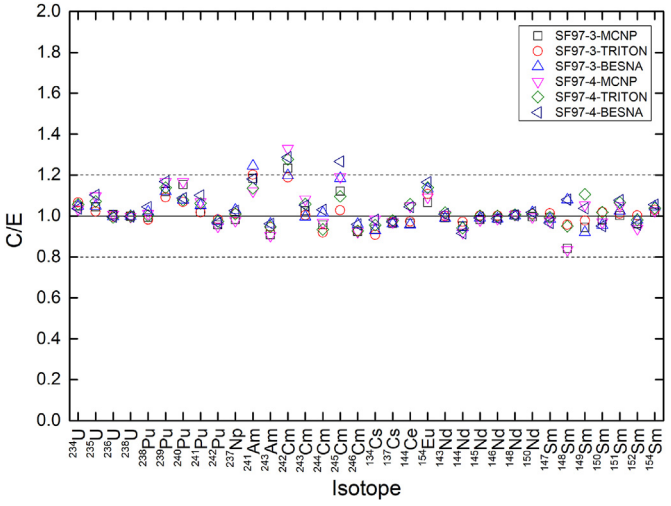

Fig. 6. Comparison of C/E ratios for samples 3 and 4 of fuel rod SF97.

predictor-corrector scheme and with the conventional CE/CM scheme using CRAM is represented as

$$R(\%) = \max_i \left| \frac{N^i_{MODIFIED} - N^i_{CONVENTIONAL}}{N^i_{CONVENTIONAL}} \right| .100\% \qquad (22)$$

where N^i represents the nuclide atomic density of nuclide i.

The maximum relative discrepancies for the measured nuclides between these two approaches used in BESNA for ten fuel samples from Takahama-3 PWR are presented in Table 4, which shows the maximum discrepancies for these cases are less than 0.6%. The comparison of computing times between these two approaches is given in Fig. 8, where the computing times are normalized by the case using the conventional CE/CM scheme without substep calculations ($nsub = 1$). The results in Fig. 8 showed that the modified approach gives a considerable reduction in computing times compared to the traditional CE/CM approach, and the speedup increases as the number of substeps increases. From the results

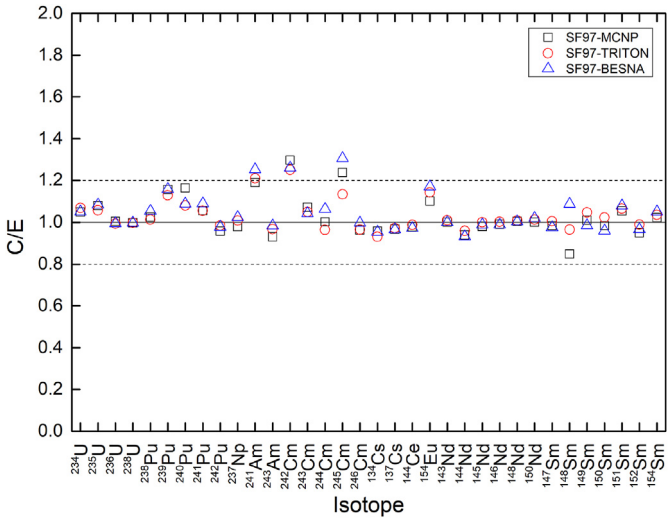

Fig. 7. Comparison of the mean C/E ratios for SF97 samples.

Table 4
Maximum discrepancy (%) between CE/CM scheme approaches in BESNA for Takahama-3 PWR fuel samples.

Fuel rod	Sample	R(%)
SF95	1	0.57
	2	0.53
	3	0.56
	4	0.56
	5	0.52
SF97	2	0.40
	3	0.42
	4	0.49
	5	0.51
	6	0.44

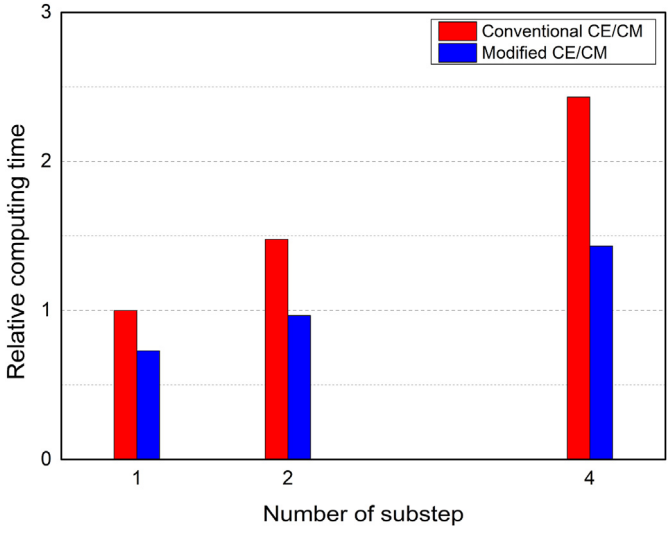

Fig. 8. Comparison of relative computing time with CE/CM schemes.

presented in Table 4 and Fig. 8, it was shown that the modified CE/CM approach can provide reliable depletion results with remarkable computational savings in this problem.

3.3. Validation of decay heat calculation in BESNA

The capability of BESNA in decay heat calculation is validated against the decay heat measured data of the Ringhals 3 PWR fuel assemblies, which were carried out by the Swedish interim storage facility, CLAB [27]. The decay heat measurements were performed for 16 FAs with the assembly IDs presented in Table 5, where the initial enrichments, discharged burnups, and cooling time are also summarized. Among these FAs, the decay heat for the ones with the ID 5A3 was measured three times in 2003 and two times in 2004. The documentation [27] reports the average values of decay heat measurements in each year.

The decay heat calculations in BESNA were performed by following the operation data in benchmark documentation [27] using the effective one-group cross section libraries generated by MCNP6 for different enrichments and burnups. The decay heat measurement and calculation results with BESNA are summarized in Table 6, where the relative and absolute discrepancies of BESNA calculation compared to the measurement results are presented. The measurement uncertainties in Table 6 are obtained by linear interpolation from the measurement uncertainties at 250 W and 900 W, which were reported in the benchmark documentation. The relative discrepancies of the decay heats calculated by BESNA compared to the measured results are about 2%, which may be resulted from the use of the general library in BESNA for all the FAs without generating the fuel assembly-specific library with detailed boron concentration in each cycle for each FA. However, these discrepancies are within the measurement uncertainties for all the considered FAs, which demonstrates the reliability of BESNA in decay heat calculations.

3.4. Verification of radiation source term estimations in BESNA

In this subsection, the neutron and gamma emission rates including spectra from BESNA are verified by comparing them with those estimated with SCALE6.2/ORIGEN for a pin-cell model. The photon and neutron source terms are calculated by BESNA for seven cases with various burnups and cooling times as listed in Table 7, and with the initial fuel compositions taken from the previous homogeneous problem in Sec. 3.1. In this verification calculations with SCALE6.2/ORIGEN, the effective one-group cross sections were produced with the SCALE6.2/TRITON.

The neutron and photon emission rates given in Table 7 show good agreements between BESNA and SCALE/ORIGEN, where the relative discrepancies between these codes are less than 1% for photon and about 3% for neutron intensities. The discrepancies in neutron emission rate for cases 1 and 2 are less than 1% but increase as the discharged burnup increases, up to 3.4% at the burnup of 55

Table 5
Decay heat measurement data for Ringhals 3 PWR fuel assemblies.

Assembly ID	Enrichment (wt.%)	Burnup (GWd/tHM)	Decay time (days)
2A5	2.1	20.11	7297
5A3	2.1	19.70	6972–7304
0C9	3.1	38.44	6551
1C2	3.1	33.32	6559
1C5	3.1	38.48	6593
2C2	3.1	36.58	6550
3C1	3.1	36.57	6545
3C4	3.1	38.45	6544
3C5	3.1	38.37	6543
3C9	3.1	36.56	6552
4C4	3.1	33.33	6572
4C7	3.1	38.37	6549
0E2	3.1	41.63	5823
0E6	3.1	35.99	5829
1E5	3.1	34.64	5818
5F2	3.4	47.31	4724

Table 6
Decay heat measurement and calculation results for Ringhals 3, PWR assemblies.

Assembly ID	Measured decay heat (W)	Measurement uncertainty (W)	Calculation decay heat (W)	C/E - 1 (%)	|C−E| (W)
2A5	233.8	8.96	234.79	0.42	0.99
5A3*	239.3	9.04	232.93	-2.66	6.37
5A3**	230.6	8.91	229.38	-0.53	1.22
0C9	491.2	12.76	490.63	-0.12	0.57
1C2	417.7	11.68	414.69	-0.74	3.01
1C5	499.2	12.88	490.57	-1.73	8.63
2C2	466.5	12.4	463.97	-0.54	2.53
3C1	470.2	12.45	462.94	-1.54	7.26
3C4	497.3	12.85	491.20	-1.23	6.10
3C5	501.4	12.91	491.10	-2.05	10.30
3C9	468.4	12.43	463.31	-1.09	5.09
4C4	422.0	11.74	414.69	-1.73	7.31
4C7	498.7	12.87	490.25	-1.70	8.45
0E2	587.9	14.19	575.61	-2.09	12.29
0E6	487.8	12.71	479.91	-1.62	7.89
1E5	468.8	12.43	461.30	-1.60	7.50
5F2	714.1	16.05	712.69	0.20	1.41

Table 7
Radiation source term verification results.

Case number	Discharged burnup (GWd/tHM)	Cooling time (years)	Neutron source (1/s)		Photon source (1/s)	
			BESNA	ORIGEN	BESNA	ORIGEN
1	20	10	8.07E+01	8.07E+01	2.25E+10	2.26E+10
2	30	10	5.25E+02	5.20E+02	3.34E+10	3.36E+10
3	40	10	1.54E+03	1.52E+03	4.22E+10	4.24E+10
4	50	10	4.02E+03	3.91E+03	5.25E+10	5.27E+10
5	55	10	5.90E+03	5.71E+03	5.75E+10	5.76E+10
6	55	20	4.05E+03	3.93E+03	3.99E+10	4.01E+10
7	55	50	1.36E+03	1.33E+03	1.96E+10	1.97E+10

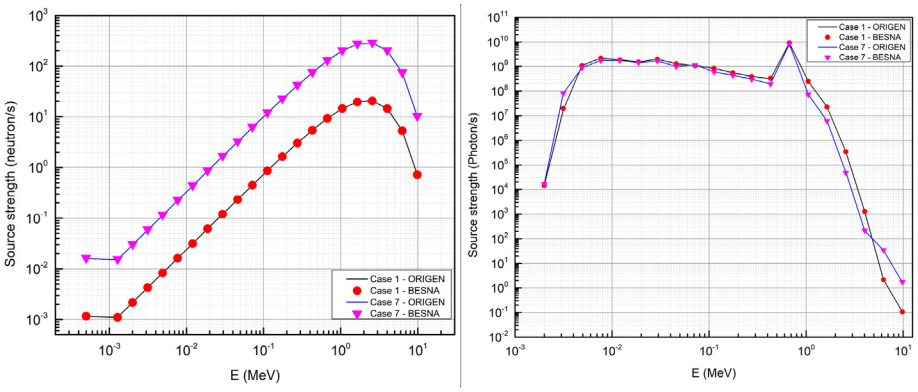

Fig. 9. Neutron (left) and photon (right) emission spectra comparison result for representative cases.

GWd/tHM. It is also noted that the discrepancy in neutron emission rate is slowly decreased as the cooling time increases, which can be seen in the last three cases. The discrepancies in neutron emission rate can be explained by the discrepancies in depletion results between two codes for ^{244}Cm, which contributes more than 95% to the spontaneous fission sources after few years of cooling. The neutron and photon spectra calculated by BESNA and SCALE/ORIGEN are compared in Fig. 9 for two representative cases (The first and the last cases), which shows that both neutron and photon spectra calculated by BESNA are consistent with those from SCALE6.2/ORIGEN.

4. Conclusions

In this paper, a new nuclear spent fuel source term calculation code BESNA was introduced and its verification and validation calculations were performed. In particular, in this paper, a new modified form of the predictor-corrector scheme was suggested for improving the computational efficiency of the conventional CE/CM scheme using CRAM in substep calculations. In this new scheme, the decay terms leading to a large norm of the depletion matrix were excluded from the corrector step, and so the corrector step calculations with the sub-step methods can be efficiently performed using the TEM method while the CRAM method is used only in the predictor step. Therefore, this approach can reduce the computing time of the conventional CE/CM scheme using CRAM. The depletion calculation in BESNA uses self-adaptive burnup-dependent effective one-group cross sections for eight types of reaction: (n,γ), $(n,2n)$ to ground or isomer state, (n,α), (n,p), (n,d), (n,t), $(n,3n)$ and $(n,fission)$. The one-group cross sections library using in BESNA is generated by MCNP6 depletion calculations for pin-cell and fuel assembly models. The cross section for the reactions producing the products at the isomer state are calculated by

combining the 63-group fluxes from MCNP6 at various burnups with the branching ratios evaluated from the CINDER library.

The depletion calculation capabilities of BESNA were verified for a simple homogeneous problem by comparing the atomic number densities obtained from BESNA and ORIGEN2 with the same effective one-group cross section libraries. The results showed that our basic depletion solver using CRAM gives the correct solution of the Bateman equation with the given effective one-group cross section libraries and related data including fission product yield data. On the other hand, the validations were performed by comparing the atomic number densities estimated with BESNA with those with other depletion codes as well as comparing to the measurement data for some samples from Takahama-3 PWR fuel rods. From the validation calculations, it was found that the BESNA code gives comparable discrepancies for most actinide and fission product nuclides from the measurement data to the other reference codes using transport and depletion coupling calculation. The capability in source terms estimation of BESNA was also verified and validated through the comparisons with measurement data from Ringhals 3 PWR fuel assemblies for decay heat and with the results calculated by SCALE6.2/ORIGEN for radiation spectra. The decay heat calculation results in BESNA were estimated to be within the measurement uncertainties, while the radiation spectra from BESNA showed good agreements with the results calculated by SCALE/ORIGEN, which demonstrate the capability of BESNA in source term estimations. The computational efficiency of the modified predictor-corrector approach using CRAM and TEM in the predictor and corrector, respectively, was also evaluated through the comparisons with the traditional CE/CM approach using CRAM for practical problems with the samples from Takahama-3 PWR fuel rods. The results showed that the calculation time with the new modified CE/CM approach could be reduced by 40% with CRAM without loss of accuracy. In particular, the reduction in computing time of the new modified method increases as the number of substeps increases.

Finally, it can be concluded from the verification and validation results that the BESNA code was successfully developed and can be applied for practical problems with computational efficiency.

Declaration of competing interest

The authors declare that they have no known competing financial interests or personal relationships that could have appeared to influence the work reported in this paper.

Acknowledgments

This work was supported by the NRF (National Research Foundation of Korea) through Project No. NRF-2019M2D2A1A02057890 and by the Korea Institute of Nuclear Safety (KINS).

References

[1] J.Ch. Sublet, J.W. Eastwood, J.G. Morgan, M.R. Gilbert, M. Fleming, W. Arter, FISPACT-II: an advanced simulation system for activation, transmutation and material modeling, Nuclear Data Sheets 139 (2017) 77–137.
[2] E. Hairer, M. Roche, C. Lubich, The Numerical Solution of Differential-Algebraic System by Runge-Kutta Methods, 2006.
[3] J. Cetnar, General solution of bateman equations for nuclear transmutations, Annals of Nuclear Energy 33 (2006) 640–645.
[4] E. Tavakkoli, M. Zangian, A. Minuchehr, A. Zolfaghari, Development and Validation of ISOBURN, a new depletion code, Annals of Nuclear Energy 159 (2021), 108319.
[5] C. Moler, C.V. Loan, Nineteen Dubious Ways to Compute the Exponential of a Matrix, Twenty-Five Years Later, Society for Industrial and Applied Mathematics, 2003.
[6] A.G. Croff, A User's Manual for the ORIGEN2 Computer Code, 1980. ORNL/TM-7175.
[7] A. Yamamoto, M. Tatsumi, N. Sugimura, Numerical solution of stiff burnup equation with short half lived nuclides by the krylov subspace method, Journal of Nuclear Science and Technology 44 (2) (2007) 147–154.
[8] X. Li, J. Cai, A new Krylov subspace method based on rational approximation to solve stiff burnup equation, Annals of Nuclear Energy 118 (2018) 99–106.
[9] N. J. Higham, The scaling and squaring method for the matrix exponential revisited, Society for Industrial and Applied Mathematic 51 (4), 747-764.
[10] M. Pusa, J. Leppanen, Computing the matrix exponential in burnup calculations, Nuclear Science and Engineering 164 (2010) 140–150.
[11] M. Pusa, Rational approximations to the matrix exponential in burnup calculations, Nuclear Science and Engineering 169 (2011) 155–167.
[12] J. Leppanen, Serpent - A Continuous-Energy Monte Carlo Reactor Physics Burnup Calculation Code, 2015.
[13] B.T. Rearden, M.A. Jessee (Eds.), SCALE Code System, ORNL/TM-2005/39, Version 6.2.1, Oak Ridge National Laboratory, Oak Ridge, Tennessee, 2016.
[14] Los Alamos National Laboratory, MCNP6 User's Manual, LA-CP-13-00634, 2013.
[15] A.E. Isotalo, G.G. Davidson, T.M. Pandya, W.A. Wieselquist, S.R. Johnson, Flux renormalization in constant burnup calculations, Annals of Nuclear Energy 96 (2016) 148–157.
[16] B. Ebiwonjumi, S. Choi, M. Lemaire, D. Lee, H. Shin, Validation of lattice physics code STREAM for predicting pressurized water reactor spent nuclear fuel isotopic inventory, Annals of Nuclear Energy 120 (2018) 431–449.
[17] B. Ebiwonjumi, S. Choi, M. Lemaire, D. Lee, H. Shin, H. Lee, Verification and validation of radiation source term capabilities in STREAM, Annals of Nuclear Energy 124 (2019) 80–87.
[18] J. Jang, C. Kong, B. Ebiwonjumi, Y. Jo, D. Lee, Uncertainties of PWR spent nuclear fuel isotope inventory for back-end cycle analysis with STREAM/RAST-K, Annals of Nuclear Energy 158 (2021), 108267.
[19] S. Jafarikia, S.A.H. Feghhi, H. Afarideh, Validation of IRBURN calculation code system through burnup benchmark analysis, Annals of Nuclear Energy 37 (2010) 325–331.
[20] K. Okumura, Y. Nagaya, T. Mori, MVP-BURN, Burn-up Calculation Code Using A Continuous-Energy Monte Carlo Code MVP, Japan Atomic Energy Agency, 2005.
[21] M. Pusa, Correction to Partial Fraction Decomposition Coefficients for Chebyshev Rational Approximation on the Negative Real Axis, 2012.
[22] W.A. Wieselquist, The SCALE 6.2 ORIGEN API for High Performance Depletion, ANS MC2015, Nashville, TN, 2015.
[23] W.B. Wilson, et al., SOURCES 4A: Code for Calculating, (α n) Spontaneous Fission, and Delayed Neutron Sources and Spectra, LA-13639-MS, 1999.
[24] E.F. Shores, Data Updates for the SOURCES-4A Computer Code, LA-UR-00-5016, 2000.
[25] W.L. Wilson, T.R. England, K.A. Van Riper, Status of CINDER'90 codes and data, proceedings of the fourth workshop on simulating accelerator radiation environments (SARE4), Knoxville (1998) 14–16. September.
[26] F. Michel-Sendis, et al., SFCOMPO-2.0: an OECD NEA database of spent nuclear fuel isotopic assays, reactor design specifications, and operating data, Annals of Nuclear Energy 110 (2017) 779–788.
[27] A.B. Svensk Kärnbränslehantering, Measurements of Decay Heat in Spent Nuclear Fuel at the Swedish Interim Storage Facility, CLAB, December, 2006.